CHEMISTRY OF MATERIALS

ARTICLE

pubs.acs.org/cm

From Single Molecules to Nanoscopically Structured Materials: Self-Assembly of Metal Chalcogenide/Metal Oxide Nanostructures Based on the Degree of Pearson Hardness

Jugal Kishore Sahoo,[†] Muhammad Nawaz Tahir,[†] Aswani Yella,[†] Thomas D. Schladt,[†] Steffen Pfeiffer,[†] Bahar Nakhjavan,[†] Enrico Mugnaioli,[‡] Ute Kolb,[‡] and Wolfgang Tremel*[,†]

[†]Institut für Anorganische Chemie und Analytische Chemie, Johannes Gutenberg-Universität, Duesbergweg 10-14, D-55099 Mainz, Germany

[‡]Institut für Physikalische Chemie, Johannes Gutenberg-Universität, Welderweg 15, D-55099 Mainz, Germany

Supporting Information

ABSTRACT: A chemically specific and facile method for the immobilization of metal oxide nanoparticles onto the surface of IF-MoS_2 nested fullerenes is reported. The modification strategy is based on the chalcophilic affinity of transition metals such as Fe^{2+}/Fe^{3+}, Fe^{3+}, or Zn^{2+} as described by the Pearson HSAB concept. The binding capabilities of the 3d metals are dictated by their Pearson hardness. Pearson hard cations such as Fe^{3+} (Fe_2O_3) do not bind to the chalcogenide surfaces; borderline metals such as Fe^{2+} (Fe_3O_4) or Zn^{2+} (ZnO) bind reversibly. Pearson-soft metals like Au bind irreversibly. The immobilization of metal oxide nanoparticle colloids was monitored by transmission electron microscopy (TEM), high resolution transmission electron microscopy (HRTEM) combined with energy dispersive X-ray spectroscopy (EDX), and X-ray diffraction (XRD).

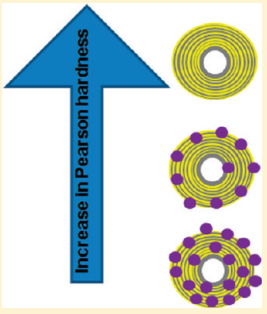

KEYWORDS: metal chalcogenide, layered compound, nanoparticle, metal oxide, reversible surface functionalization

INTRODUCTION

Current efforts and success of nanoscale science and technology are related to the fabrication of functional materials and devices in which the individual units and their spatial arrangement are engineered down to the nanometer level.[1] One promising way of achieving this goal is to assemble different nanomaterials to form hybrid nanocomposites that effectively combine the properties of different materials involved. Furthermore, the assembly of multicomponent nanomaterials from constituents with different optical, electrical, magnetic, and chemical properties can lead to novel functionalities that even surpass those of the individual components and may be tailored for specific applications. The generation of such hybrid nanocomposites could represent a new approach to nanoscale building blocks.

Surface functionalization is one of the requirements for controlling the assembly of nanoparticles to aggregates with hierarchical structure.[2] Surface chemistry is "coordination chemistry in two dimensions", i.e., most nanoparticles (e.g., metals, metal sulfides, or metal oxides) can be surface treated in a straightforward fashion using the concepts of coordination chemistry. In general, a surface ligand contains an anchor group that strongly attaches onto the surface of the regarding nanomaterial and a (long) hydrocarbon or polyether chain that confers solubility in apolar or polar solvents.[3] A terminal group (e.g., an amino group) provides connectivity to additional functional ligands. Typical anchor groups include phosphines,[4] amines,[5] thiols,[6] carboxylates,[7] phosphates,[8] or catecholates.[9] As a result, a dense ligand shell is formed around each nanoparticle, preventing particle aggregation and providing chemical protection against oxidation plus long-term solvent stability.

In contrast to most nanoparticles, inorganic nanotubes (NT-MQ_2, where M = W, Mo, Nb, and Q = S, Se)[10] and inorganic fullerenes (IF-MQ_2)[11] of layered metal chalcogenides consist of metal atoms sandwiched between two inert chalcogenide layers. These MQ_2 layers are stacked with only van der Waals contacts between them. The steric shielding of the metal atoms by the chalcogen surface layers from nucleophilic attack by oxygen or organic ligands makes chalcogenide nanoparticles highly inert and notoriously difficult to functionalize. While a covalent surface chemistry of their carbon congeners (fullerenes and nanotubes) has been established through acid-induced oxidation of the carbon nanotube surface defects,[12] the covalent surface functionalization of layered chalcogenides is *anion coordination chemistry*: metals with a high sulfur affinity, whose coordination sphere is partially blocked by chelating groups, must serve as a "glue" for anchoring organic ligands to the sulfur surface.

Some progress has been made by employing chalcophilic transition metals in combination with multi-dentate surface ligands: The 3d metals "wet" the sulfur surface of the chalcogenide nanoparticles, while the multi-dentate surface ligands partially block one hemisphere of the metal coordination environment. This steric shielding prevents an aggregation of the

Received: April 25, 2011
Revised: June 2, 2011
Published: July 06, 2011

chalcogenide nanoparticles through interparticle cross-linking.[13] This covalent attachment offers high stability in different solvents and ionic environments. An alternative strategy is to attach nanoparticles directly onto the chalcogenide nanoparticles.[14] In this case, the sulfur atoms of the chalcogenide particles outcompete the protecting ligand of the nanoparticle surface, i.e., their affinity is based on their acid/base properties or Pearson hardness,[15] which allows their attachment without the aid of linkers.

In this paper, we report a general synthetic strategy based on Pearson's HSAB (Hard Soft Acid Base) principle[16] that allows the formation of a hierarchical assembly of metal chalcogenide/metal oxide nanostructures. The binding capabilities of the 3d metals are dictated by their Pearson hardness, whereas Pearson hard cations such as Ti^{4+} (TiO_2) or Fe^{3+} (Fe_2O_3) do not bind to the chalcogenide surfaces, borderline metals such as Fe^{2+} (Fe_3O_4) or Zn^{2+} (ZnO) bind reversibly and can be detached reversibly from the chalcogenide surfaces with excess surface ligand. Pearson soft metals like gold bind irreversibly.

EXPERIMENTAL SECTION

Materials and Methods. 3-Hydroxy tyramine hydrochloride (Acros organic) and 1-hexadecanethiol (Sigma-Aldrich) were purchased and used as received without further purification. Solvents, such as toluene, chloroform, and DMF, were purchased technical grade and used as received.

Synthesis of Fe_3O_4 Nanoparticles. Fe_3O_4 nanoparticles were synthesized using a reported procedure.[17] Typically, iron(III) acetylacetonate ($Fe(acac)_3$, 150 mg) was mixed in dioctylether (10 mL) with 1,2-hexadecanediol (250 mg), oleic acid (0.06 mL), and oleylamine (0.06 mL) in a glovebox under argon. Under mechanical stirring, the reaction mixture was heated to 280 °C for 30 min. Ethanol (20 mL) was added after the reaction mixture was cooled to room temperature. A dark-brown precipitate (magnetite seeds) was acquired after centrifugation. The magnetite seeds (25 mg) were dissolved in 10 mL of dioctylether and mixed with $Fe(acac)_3$ (150 mg), 1,2-hexadecanediol (250 mg), oleic acid (0.06 mL), and oleylamine (0.06 mL). The mixture was heated to 280 °C for 30 min under mechanical stirring. After the mixture was cooled to room temperature, it was treated with ethanol, and a dark-brown material was precipitated from the solution. The product was dissolved in hexane and reprecipitated with ethanol to yield uniform Fe_3O_4 nanoparticles.

Synthesis of ZnO Colloids. A batch of ZnO colloids were synthesized by dissolving 110 mg (0.5 mmol) of $Zn(CH_3COO)_2\,2H_2O$ in 25 mL of ethanol with sonication for 15 min at 0 C. To the above solution was added 21 mg (0.5 mmol) of $Li(OH)x3H_2O$, and sonication was continued for another 15 min at the same temperature. A stable and optically transparent dispersion of ZnO nanoparticles was obtained.

Synthesis of Fe_2O_3 Nanoparticles. Fe_2O_3 nanoparticles were prepared following the reported procedure.[18] Typically, $Fe(CO)_5$ (0.2 mL, 1.52 mmol) was injected under vigorous stirring into a solution containing 0.91 g of lauric acid (4.56 mmol), 7 mL of octyl ether, and 0.57 g of $(CH_3)_3NO$ (7.60 mmol) at 100 °C in an argon atmosphere. As soon as $Fe(CO)_5$ was injected into the mixture, the temperature rose to 120 °C, and the solution became dark-red, which indicated the successful oxidation of $Fe(CO)_5$. The reaction mixture was stirred for 1 h at 120 °C, and the solution was slowly heated to reflux. The color of the solution gradually turned black, indicating that nanoparticles were formed. After refluxing for 1 h, the solution was cooled to room temperature, and a black precipitate was obtained upon adding excess ethanol and centrifuging. The precipitate can be easily redispersed in toluene.

Synthesis of IF-MoS_2. IF-MoS_2 was synthesized as described in ref 11c.

Synthesis of MnO, TiO_2, Au Nanoparticles. MnO,[19] TiO_2,[20] and Au[23] nanoparticles were synthesized using reported procedures.

Binding of Metal (Au) and Metal Oxide (MnO, Fe_3O_4, ZnO, Fe_2O_3, TiO_2) Nanoparticles onto IF-MoS_2. In a typical experiment, 4 mg of IF-MoS_2 were dispersed in 5 mL toluene or ethanol (depending upon the nanoparticles to be immobilized) by sonicating the sample for 5−7 min. The solution was degassed under argon for 10−15 min. In another centrifuge vial, 8 mg of nanoparticles were dissolved in 5 mL of toluene (MnO, Fe_3O_4, Fe_2O_3) or ethanol (ZnO, TiO_2, Au), respectively. Subsequently, the solution was added dropwise to the degassed mixture of IF-MoS_2 in toluene or ethanol over a period of 5−7 min. Subsequently, the reaction mixture was degassed again under argon for 5 min and put in a shaker for 6 h at room temperature (RT). After the reaction was complete, the unbound nanoparticles were washed out by centrifuging the sample thrice at 4000 rpm for 10 min. Finally, the functionalized IF-MoS_2 was characterized by TEM/HRTEM combined with EDX. Samples for TEM were prepared by putting 1−2 drops of dispersed sample on a copper TEM grid followed by drying.

Reversibility Experiments. In a typical experiment, 10 mg of the IF-MoS_2/metal oxide nanocomposite was taken in a 50 mL flask and dispersed with 5 mL of DMF by sonication followed by degassing the mixture in argon. In another flask, 40 mg of 3-hydroxytyramine hydrochloride (dopamine) was taken and dissolved in 10 mL of DMF. The dopamine solution was added dropwise to the mixture of the IF-MoS_2@metal oxide nanocomposite over a period of 10 min. The reaction mixture was heated to 60 °C and stirred overnight. After the reaction was complete, the reaction mixture was washed by centrifuging the sample thrice at 4000 rpm for 10 min. The recycled IF-MoS_2 can be used for further functionalization with fresh metal oxide nanoparticles. Similarly, the metal oxide was removed from the surface of MoS_2 by using dopamine in DMF as a competing ligand as described above. The reaction was monitored by transmission electron microscopy. A similar procedure was used for the reversibility experiment of other metal oxide nanoparticles and IF-MoS_2. For the reversibility experiment with IF-MoS_2/Au nanocomposites, hexadecanethiol instead of dopamine was used as competing ligand.

Characterization. *TEM Analysis and Characterization of the Products.* Transmission electron microscopy (TEM) was carried out on a Philips EM420 instrument with a twin lens and a Philips CM12 with a twin lens at an acceleration voltage of 120 kV. High resolution images were taken with a Philips FEI TECNAI F30 ST electron microscope (field-emission gun, 300 kV extraction voltage) equipped with an Oxford EDX (energy-dispersive X-ray) spectrometer with a Si/Li detector and an ultrathin window for elemental analysis. Samples for TEM measurements were prepared from ethanolic suspensions of the samples on carbon-coated Cu grids. Three drops of the ultrasonicated suspension were administered on a Cu grid coated with FORMVAR polymer and an amorphous carbon layer.

RESULTS AND DISCUSSION

Immobilization of Metal Oxide Nanoparticles on IF-MoS_2 Surfaces. The constituent IF-MoS_2 nanoparticles were prepared following a MOCVD approach.[11c] MnO,[19] Fe_2O_3,[18] and Fe_3O_4[17] as well as TiO_2[20] and Au[21] nanoparticles were synthesized by wet-chemical methods. These constituent nanoparticles were characterized by TEM as shown in Figure 1 and Figure S1 (Supporting Information). The X-ray diffractograms of MnO, Fe_2O_3, and Fe_3O_4 are provided in Figure S2 (Supporting Information). The functionalization scheme of the IF-MoS_2 nanoparticles is illustrated in Scheme 1. In a typical experiment, IF-MoS_2 was dispersed under sonication in toluene followed by addition of the metal oxide nanoparticles to the dispersion of the

chalcogenide nanoparticles. The product, metal oxide functionalized IF-MoS_2, was characterized by TEM and EDX.

Panel (a) of Figure 2 shows a TEM overview image of MnO nanoparticles surface-bound to IF-MoS_2. The layered structure of IF-MoS_2 with an interlayer separation of 0.63 nm is apparent from the HRTEM micrograph in panel (b) of Figure 2. The affinity of MnO (with the Pearson borderline metal Mn^{2+}) to IF-MoS_2 (with Pearson soft sulfide anions) is large enough to ensure the formation of a full MnO monolayer (with a number of defects) on the chalcogenide surface. The surface of the MnO particles is blocked by the oleic acid capping ligands from the particle synthesis, which prevents a self-aggregation of the MnO particles. The surface binding of the MnO particles is assumed to proceed by a "nucleophilic" substitution of the oleic acid capping ligands by the chalcogenide sulfur atoms. The functionalization was confirmed from EDX spectrum, which shows the presence of Mo, S, Mn, and O in the nanocomposites. The Cu signals are from the Cu TEM grids.

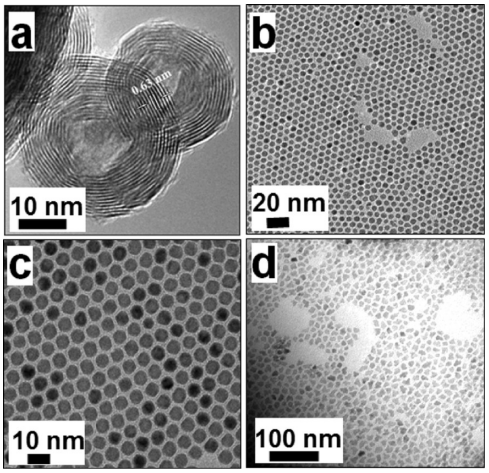

Figure 1. Electron microscopy images of as-synthesized nanoparticles. (a) IF-MoS_2, (b) Fe_2O_3, (c) MnO, (d) Fe_3O_4.

Scheme 1. Schematic Representation of the Reversible Immobilization of Metal Oxide and Irreversible Binding of Au Nanoparticles onto IF-MoS_2

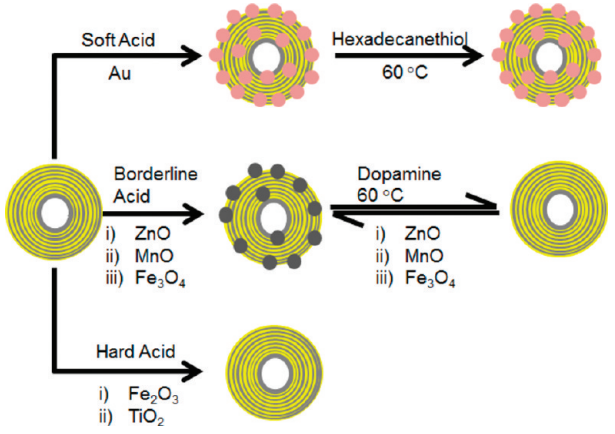

Panel (a) of Figure 3 shows a TEM overview micrograph of Fe_3O_4 functionalized IF-MoS_2. The corresponding HRTEM image is provided in panel (b) of Figure 3, showing the interlayer separation of the IF-MoS_2 particles and the lattice fringes of the "satellite" Fe_3O_4 nanoparticles. The EDX spectrum in panel (c) of Figure 3 shows signals of Mo, S, Fe, and O together with the Cu signals of the Cu grid. According to the Pearson hardness scale in Table 1, magnetite containing Fe^{3+} and Fe^{2+} at the octahedral sites and Fe^{3+} at the tetrahedral sites of the spinel lattice should have a lower affinity to the surface sulfur atoms of IF-MoS_2. Although this trend could not be substantiated by a competitive detachment experiment with Fe_3O_4 and MnO, it is supported by a comparison of the surface binding of maghemite (Fe_2O_3) and anatase (TiO_2). The Pearson hardness[15,16] of the constituent metals Fe^{3+} (13.1 eV) and Ti^{4+} (>$\eta(Sc^{3+})$ 24.6 eV) prevent a binding of maghemite and anatase to the IF-MoS_2 surface, i.e., the harder capping ligands of the surfaces of the Fe_2O_3 and TiO_2 particle outcompete the soft sulfur atoms, i.e., no substitution of these ligands by sulfur is possible. Figure S4 (Supporting Information) shows the absence of binding of TiO_2 to the chalcogenide particle. The binding of TiO_2 nanoparticles to the incompatible chalcogenide surface could, however, be achieved with the aid of specially designed surface ligands containing tailor-made anchor groups for the chalcogenide and oxide surfaces.[22]

A comparison of the binding tendencies of the iron oxides is given in Figure 4, showing surface-bound Fe_3O_4 (IF-MoS_2@Fe_3O_4) and unbound Fe_2O_3 and IF-MoS_2 nanoparticles. The magnetic Fe_3O_4 and Fe_2O_3 nanoparticles are attracted by the permanent magnet. Whereas the sample containing the surface-bound magnetite nanoparticles (left) becomes transparent by attraction of the composite IF-MoS_2@Fe_3O_4 to the magnet, the IF-MoS_2 particles remain unbound and well dispersed, thereby leaving a turbid sample (right).

Similar experiments were carried out to study the binding affinity of other metal oxide particles such as ZnO to IF-MoS_2. ZnO nanoparticles bind strongly to the surface of IF-MoS_2 or WS_2 nanotubes.[23] Figure 5 shows the monolayer coverage of ZnO colloidal particles on the surface of IF-MoS_2 nanoparticles.

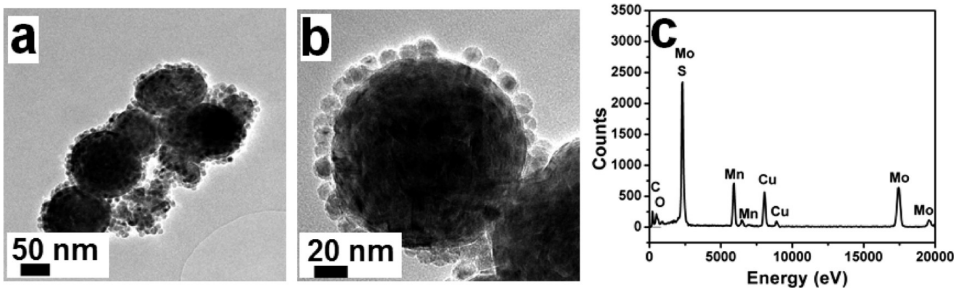

Figure 2. (a) TEM overview and (b) HRTEM image of MnO coated IF-MoS_2 nanoparticles. (c) EDX spectrum showing the presence of Mo and S as well as Mn and O. The Cu signal is due to the Cu TEM grid.

dx.doi.org/10.1021/cm201178n |*Chem. Mater.* 2011, 23, 3534–3539

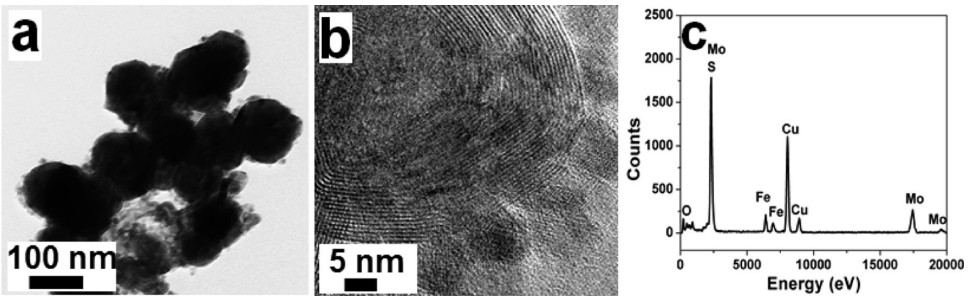

Figure 3. (a) TEM overview and (b) HRTEM images of Fe_3O_4 nanoparticles bound onto IF-MoS_2 particles. (c) EDX spectrum showing the presence of Mo and S as well as Fe and O. The Cu signal is due to the Cu TEM grid.

Table 1. Pearson Hardness[15,16] of transition metal species used for the assembly of metal oxide or metal particles on chalcogenide nanoparticles

cations	Pearson hardness η (eV)
Fe^{3+}	13.1
Zn^{2+}	10.8
Mn^{2+}	9.3
Fe^{2+}	7.2
Au	3.5

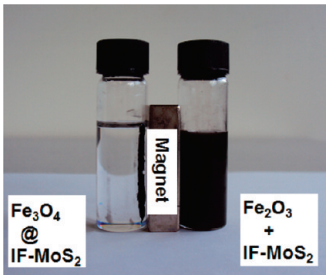

Figure 4. Digital image of surface-bound Fe_3O_4 (IF-MoS_2@Fe_3O_4) and unbound Fe_2O_3 nanoparticles. The magnetic nanoparticles are attracted by the permanent magnet. Whereas the sample containing the surface-bound magnetite nanoparticles (left) becomes transparent through the attraction by the magnet, the unbound IF-MoS_2 particles remain dispersed leaving a turbid sample (right).

The binding of Zn^{2+} cations to sulfide surfaces is not unexpected because it is well-known that Zn^{2+} in aqueous solutions readily forms ZnS precipitates in the presence of sulfide (or H_2S). Likewise, solid ZnO can be sulfidized easily with H_2S. Au as one of the softest metals (Pearson hardness 3.5 eV) is known to be highly chalcophilic; this property of gold and the coinage metals is the basis of the established SAMs[24] and a very rich chalcogenide chemistry.[26] As a consequence, Au nanoparticles strongly bind to IF-MoS_2 as illustrated in Figure S3 (Supporting Information).

Reversible Detachment of Metal Oxide (MnO, Fe_3O_4, ZnO) Nanoparticles from IF-MoS_2 Surfaces. The IF-MoS_2 surface-bound metal oxide nanoparticles can be functionalized selectively with various surface ligands. In this process, either the original (e.g., oleic acid) capping ligands or the chalcogenide surface ligands are replaced by competing ligands that can have a higher affinity for the metal ions Mn^{2+}, Fe^{2+} and Zn^{2+}. However, surface ligands can be replaced by competing ligands with a lower binding affinity under equilibrium reactions, as long as there is a sufficiently large excess of the competing ligand.

Each of the metal ions Mn^{2+}, $Fe^{2+/3+}$, and Zn^{2+} bound to the IF-MoS_2 surface can be functionalized highly efficiently and selectively with "noninnocent" redox-active ligands such as catechol.[9] Unlike most ligands used in inorganic chemistry, such as amines or phosphines, redox-active, or "noninnocent," ligands[26] have more energetically accessible levels that allow redox reactions to change their charge state. As a result, many coordination compounds with noninnocent ligands are very stable, which makes them useful in analytical chemistry.[27] Catecholates or diimines have a distinctive ability to form noninnocent surface species which makes them powerful anchor groups for nanoparticle functionalization.[28] In this process, the oleic acid capping ligands are replaced by the free catechol ligand. Due to its chelating properties, catechol can compete highly successfully with sulfur for surface metal atoms. In particular hard acids such as Fe^{3+} (or Al^{3+} and Ti^{4+}) prefer coordination to donor groups such as hydroxamate, phenolate, and catecholate.[29] The catecholate ligands form unstrained and unsaturated five-membered ring chelate systems with surface metal atoms via negatively charged oxygen (or nitrogen) atoms. Thus, ligands with oxygen donors form stable surface complexes with trivalent or tetravalent metals, whereas those with softer donor atoms such as nitrogen (intermediate) or sulfur (soft) also favor soft metals such as Zn^{2+}.[30]

Due to their chelating properties, catechol type ligands can compete successfully with sulfur atoms of the fullerene surface for the surface metal atom. Solvation is an important factor that determines the surface binding of the oxide nanoparticles. As the solvation increases with increasing the temperature, we used a slightly elevated temperature of 60 °C to remove the surface-bound oxide nanoparticles from the chalcogenide surface in the presence of dopamine as chelating ligand for the metal oxide nanoparticles. Using this strategy, MnO, Fe_3O_4, and ZnO particles could be detached completely from the chalcogenide particles. However, without addition of the competing ligand, the recovery of the chalcogenide nanoparticles was not possible.

For attempts to detach gold nanoparticles from IF-MoS_2, monodentate thiols (e.g., hexadecanethiol) were used as the competing ligands. However, Au nanoparticles could not be detached from the IF-MoS_2 particle surfaces.

Our results are summarized in Scheme 1. Whereas oxides of soft and borderline metals are chemisorbed easily to the surface sulfur atoms, oxides of the hard metals have a much lower tendency for binding. The catechol-type ligands bind efficiently to hard or borderline metals (such as Ti^{4+} Fe^{3+}, Al^{3+}, Mn^{2+} etc.). As a result, the binding of chalcogenide nanoparticles and

dx.doi.org/10.1021/cm201178n |*Chem. Mater.* 2011, 23, 3534–3539

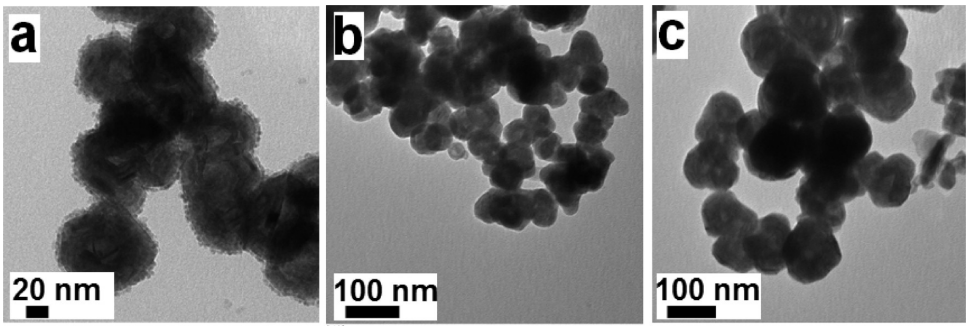

Figure 5. (a) TEM micrograph of IF-MoS_2 nanoparticles with a monolayer of surface-bound ZnO particles. (b) IF-MoS_2 nanoparticles after detachment of the ZnO particles or (c) Fe_3O_4 particles with catecholate ligands.

catechol-type ligands to surface metal atoms of borderline metal oxides is a dynamic equilibrium reaction, whose position depends on the reactants and temperature. By increasing the reaction temperature to 60 °C, catechol is a preferred surface ligand for the metal oxide particles. It displaces the surface sulfur atoms of IF-MoS_2 from the oxide particles leaving unfunctionalized and separated IF-MoS_2 particles. The addition of new metal oxide nanoparticles to IF-MoS_2 leads to a partial replacement of the oleate surface ligands by the surface sulfur atoms of IF-MoS_2 and a concomitant binding of metal oxide nanoparticles to the chalcogenide surface. This cycle can be repeated several times. The recycled chalcogenide nanoparticles can be reused.

The HSAB model has its basis in arguments related to bonding strength. It is applied for systems where kinetic control, entropy of adduct formation, solvation effects (enthalpic and entropic), ion-pairing effects (enthalpic and entropic), or lattice energy effects (enthalpic and entropic) are large and even dominant. When HSAB considerations are employed, it is implied that the soft−soft (covalent) or hard−hard (ionic) interactions dominate the chemistry, i.e., that the reactions are either orbital or charge controlled.

Thus, the reversible binding of MnO, Fe_3O_4, and ZnO nanoparticles to the chalcogenide surface can be attributed to the relative hardness of the metal cations of the respective metal oxide nanoparticles. The hardness of Au(0) is 3.5 eV, whereas the corresponding values for Mn^{2+}, Fe^{2+}, Fe^{3+}, and Zn^{2+} are 9.3, 7.2, 13.1, and 10.8 eV, respectively.[15,16] Therefore, the binding of the divalent metals is reversible, and the trivalent metal does not bind to the chalcogenide surface. The binding of chalcophilic Au is irreversible.[31]

In summary, we have demonstrated a generalized strategy for the functionalization of chalcogenide particles using metal oxide and metal nanoparticles. In their pristine form, chalcogenide nanoparticles are highly inert and difficult to functionalize. The Pearson hardness of the different metal cations was used as a basis for the binding of the metal oxides to the chalcogenide surface. Although small molecules like oxygen may adsorb to surface defects, the immobilization of metal oxides nanoparticles is dependent on the Pearson hardness of the respective metal cations as evident by the binding trend and binding density of the different metal oxides. The "self-assembled" hybrid architecture can incorporate various different selective nanoparticle−substrate interactions based on well-known surface chemistrys, and it may be generalized for various layered chalcogenide nanoparticles and transition metal and main group oxides. This assembly technique offers benefits for low-cost and low-waste manufacturing, and such methods are becoming increasingly important in the development of green nanofabrication strategies.

The functionalization of the chalcogenide nanoparticles opens new fields for this class of materials which have been pursued actively during the past few years for the related carbon nanotubes and oxide materials: (i) The dispersion of nanoparticles, e.g., for the integration in composites, is of interest because of the exceptional mechanical properties of chalcogenide nanoparticles. (ii) It allows the fabrication of thin films by surface binding of chalcogenide particles to oxide surfaces, which might allow their use as lubricants on seemingly incompatible ceramic materials. (iii) Finally, it enables the functionalization of chalcogenide nanoparticles for the attachment of electronically active components (e.g., metal and semiconductors nanoparticles, light harvesting ligands for solar cell applications).

■ ASSOCIATED CONTENT

Supporting Information. Synthetic details, X-ray diffraction, TEM images of as-synthesized Au nanoparticles, TiO_2 nanoparticles, and ZnO colloids, and IF-MoS_2 functionalized with Au nanoparticles. This information is available free of charge via the Internet at http://pubs.acs.org/.

■ AUTHOR INFORMATION

Corresponding Author

*Phone: +49 6131 392-5135; Fax: +49 6131 392-5605; E-mail: tremel@uni-mainz.de.

■ ACKNOWLEDGMENT

This work was supported by the Deutsche Forschungsgemeinschaft (DFG). A.Y. is a recipient of a fellowship from POLYMAT, the Graduate School of Excellence of the State of Rhineland-Palatinate. B.N. received a fellowship from the Deutscher Akademischer Austauschdienst (DAAD). T. D. Schladt is recipient of a Carl-Zeiss fellowship. We acknowledge support for the Electron Microscopy Center in Mainz (EZMZ) from the Center for Complex Matter (COMATT) and the SFB 625. We are indebted to Dr. Martin Panthöfer for helpful discussions.

■ REFERENCES

(1) (a) Cozzoli, P. D.; Pellegrino, T.; Manna, L. *Chem. Soc. Rev.* **2006**, *35*, 1195. (b) Zeng, H.; Sun, S. *Adv. Funct. Mater.* **2008**, *18*, 391. (c) McGuire, J. A.; Joo, J.; Pietryga, J. M.; Schaller, R.; Klimov, V. I. *Acc. Chem. Res.* **2008**, *41*, 1810.

(2) (a) Pileni, M.-P. *Nanocrystals Forming Mesoscopic Structures*; Pileni, M.-P., Ed.; Wiley VCH: Weinheim, Germany, 2005. (b) Balazs, A. C.; Emrick, T.; Russell, T. P. *Science* **2006**, *314*, 1107. (c) Kang, H.; Detcheverry, F. A.; Mangham, A. N.; Stoykovich, M. P.; Daoulas, K. C.; Hamers, R. J.; Müller, M.; de Pablo, J. J.; Nealey, P. F. *Phys. Rev. Lett.* **2008**, *100*, 148303. (d) Talapin, D. V.; Lee, J.-S.; Kovalenko, M. V.; Shevchenko, E. V. *Chem. Rev.* **2010**, *110*, 389–458.

(3) Ribas Gispert, J. *Coordination Chemistry*, 1st ed.; Wiley-VCH: Weinheim, Germany, 2008.

(4) (a) Ramirez, E.; Jansat, S.; Philippot, K.; Lecante, P.; Gomez, M.; Masdeu-Bulto, A. M.; Chaudret, B. J. *Organomet. Chem.* **2004**, *689*, 4601. (b) Woehrle, G. H.; Hutchison, J. E. *Inorg. Chem.* **2005**, *44*, 6149.

(5) Warner, M. G.; Hutchison, J. E. In *Synthesis, Functionalization and Surface Treatment of Nanoparticles.* ; Baraton, M.-I., Ed.; American Scientific Publishers : Stevenson Ranch, CA, 2003; p 67.

(6) (a) Brust, M.; Walker, M.; Bethell, D.; Schiffrin, D. J.; Whyman, R. *J. Chem. Soc. Chem. Commun.* **1994**, 801. (b) Bartz, M.; Küther, J.; Nelles, G.; Weber, N.; Seshadri, R.; Tremel, W. *J. Mater. Chem.* **1999**, *9*, 1121–1125.

(7) (a) O'Regan, B.; Grätzel, M. *Nature* **1991**, *353*, 737–740. (b) Brust, M.; Fink, J.; Bethell, D.; Schiffrin, D. J.; Kiely, C. *J. Chem. Soc. Chem. Commun.* **1995**, 1655. (c) Doty, R. C.; Tshikhudo, T. R.; Brust, M.; Fernig, D. G. *Chem. Mater.* **2005**, *17*, 4630. (d) Jiang, H.; Moon, K.-S.; Li, Y.; Wong, C. P. *Chem. Mater.* **2006**, *18*, 2969.

(8) (a) Subbiah, A.; Pyle, D.; Rowland, A.; Huang, J.; Narayanan, R. A.; Thiyagarajan, P.; Zon, J.; Clearfield, A. *J. Am. Chem. Soc.* **2005**, *127*, 10826. (b) Adden, N.; Gamble, L. J.; Castner, D. G.; Hoffmann, A.; Gross, G.; Menzel, H. *Langmuir* **2006**, *22*, 8197. (c) Viornery, C.; Chevolot, Y.; Leonard, D.; Aronsson, B.-O.; Pechy, P.; Mathieu, H. J.; Descouts, P.; Graetzel, M. *Langmuir* **2002**, *18*, 2582. (d) Hoque, E.; DeRose, J. A.; Kulik, G.; Hoffmann, P.; Mathieu, H. J.; Bhushan, B. *J. Phys. Chem. B* **2006**, *110*, 10855. (e) White, M. A.; Johnson, J. A.; Koberstein, J. T.; Turro, N. J. *J. Am. Chem. Soc.* **2006**, *128*, 11356.

(9) (a) Waite, J. H.; Tanzer, M. L. *Science* **1981**, *212*, 1038. (b) Xu, C.; Xu, K.; Gu, H.; Zheng, R.; Liu, H.; Zhang, X.; Guo, Z.; Xu, B. *J. Am. Chem. Soc.* **2004**, *126*, 9938. (c) Tahir, M. N.; Eberhardt, M.; Theto, P.; Faiss, S.; Janshoff, A.; Gorelik, T.; Kolb, U.; Tremel, W. *Angew. Chem.* **2006**, *118*, 922. *Angew. Chem., Int. Ed.* **2006**, *45*, 908.

(10) (a) Margulis, L.; Salitra, G.; Tenne, R.; Talianker, M. *Nature* **1993**, *365*, 113. (b) Therese, H. A.; Li, J.; Kolb, U.; Tremel, W. *Solid State Sci.* **2005**, *7*, 67.

(11) (a) Feldman, Y.; Wasserman, E.; Srolovitz, D. J.; Tenne, R. *Science* **1995**, *267*, 222. (b) Tenne, R.; Homyonfer, M.; Feldman, Y. *Chem. Mater.* **1998**, *10*, 3225. (c) Etzkorn, J.; Therese, H. A.; Rocker, F.; Berntsen, N.; Kolb, U.; Tremel, W. *Adv. Mater.* **2005**, *17*, 2372–2375. (d) Zink, N.; Pansiot, J.; Kieffer, J.; Therese, H. A.; Panthöfer, M.; Rocker, F.; Kolb, U.; Tremel, W. *Chem. Mater.* **2007**, *19*, 6391.

(12) Hirsch, A.; Vostrowsky, O. *Top. Curr. Chem.* **2005**, *245*, 193.

(13) (a) Tahir, M. N.; Eberhardt, M.; Zink, N.; Therese, H. A.; Kolb, U.; Theato, P.; Tremel, W. *Angew. Chem.* **2006**, *118*, 4927. *Angew. Chem., Int. Ed.* **2006**, *45*, 4809. (b) Tahir, M. N.; Yella, A.; Sahoo, J. K.; Natalio, F.; Kolb, U.; Jochum, F.; Theato, P.; Tremel, W. *Isr. J. Chem.* **2010**, *50*, 500–505. (c) Sahoo, J. K.; Tahir, M. N.; Yella, A.; Branscheid, R.; Kolb, U.; Tremel, W. *Langmuir* **2011**, *27*, 385–391.

(14) Sahoo, J. K.; Tahir, M. N.; Yella, A.; Schladt, T. D.; Mugnaioli, E.; Kolb, U.; Tremel, W. *Angew. Chem.* **2010**, *120*, 7741. *Angew. Chem., Int. Ed.* **2010**, *49*, 7578.

(15) (a) Parr, R. G.; Pearson, R. G. *J. Am. Chem. Soc.* **1983**, *105*, 7512. (b) Pearson, R. G. *Chemical Hardness. Applications from Molecules to Solids*, Wiley-VCH, Weinheim, Germany, 1997.

(16) (a) Pearson, R. G. *J. Am. Chem. Soc.* **1963**, *85*, 3533. (b) Pearson, R. G. *J. Chem. Educ.* **1968**, *45*, 581. (c) Pearson, R. G. *J. Chem. Educ.* **1968**, *45*, 643.

(17) Zheng, R.; Gu, H.; Xu, B.; Fung, K. K.; Zhang, X.; Ringer, S. P. *Adv. Mater.* **2006**, *18*, 2418.

(18) Hyeon, T.; Lee, S. S.; Park, J.; Chung, Y.; Na, H. B. *J. Am. Chem. Soc.* **2001**, *123*, 12798.

(19) Schladt, T. D.; Graf, T.; Tremel, W. *Chem. Mater.* **2009**, *21*, 3183.

(20) Tahir, M. N.; Theato, P.; Oberle, P.; Melnyk, G.; Kolb, U.; Stepputat, M.; Tremel, W. *Langmuir* **2006**, *22*, 5209.

(21) Küther, J.; Seshadri, R.; Nelles, G.; Butt, H.-J.; Knoll, W.; Tremel, W. *Adv. Mater.* **1998**, *10*, 401.

(22) (a) Tahir, M. N.; Eberhardt, M.; Therese, H. A.; Kolb, U.; Theato, P.; Mueller, W. E. G.; Schroeder, H. C.; Tremel, W. *Angew. Chem.* **2006**, *118*, 4921. *Angew. Chem., Int. Ed.* **2006**, *45*, 4803. (b) Tahir, M. N.; Zink, N.; Eberhardt, M.; Therese, H. A.; Kolb, U.; Theato, P.; Tremel, W. *Small* **2007**, *3*, 829. (c) Tahir, M. N.; Natalio, F.; Therese, H. A.; Yella, A.; Metz, N.; Shah, M. R.; Mugnaioli, E.; Berger, R.; Theato, P.; Schroeder, H. C.; Müller, W. E. G.; Tremel, W. *Adv. Funct. Mater.* **2009**, *19*, 285.

(23) Tahir, M. N.; Yella, A.; Therese, H. A.; Mugnaioli, E.; Panthöfer, E.; Khan, H. U.; Knoll, W.; Kolb, U.; Tremel, W. *Chem. Mater.* **2009**, *21*, 5382.

(24) Ulman, A. *Chem. Rev.* **1996**, *96*, 1533. (b) Love, J. C.; Estroff, L. A.; Kriebel, J. K.; Nuzzo, R. G.; Whitesides, G. M. *Chem. Rev.* **2005**, *105*, 1103.

(25) Krebs, B.; Henkel, G. *Angew. Chem.* **1991**, *103*, 785. *Angew. Chem., Int. Ed. Engl.* **1991**, *30*, 769.

(26) Jørgensen, C. K. *Coord. Chem. Rev.* **1966**, *1*, 164.

(27) Umland, F.; Wünsch, G. *Charakteristische Reaktionen Anorganischer Stoffe*, 2nd ed.; Aula Verlag, Wiesbaden, 1991.

(28) (a) Pierpont, C. G.; Lange, C. W. *Prog. Inorg. Chem.* **1994**, *41*, 331. (b) Chaudhuri, P.; Verani, C. N.; Bill, E.; Bothe, E.; Weyhermüller, T.; Wieghardt, K. *J. Am. Chem. Soc.* **2001**, *123*, 2213. (c) Pierpont, C. G. *Coord. Chem. Rev.* **2001**, *216−217*, 99. (d) Pierpont, C. G. *Coord. Chem. Rev.* **2001**, *219−221*, 415.

(29) Kaim, W.; Schwederski, B. *Coord. Chem. Rev.* **2010**, *254*, 1580.

(30) Hancock, R. D.; Martell, A. E. *Chem. Rev.* **1989**, *89*, 1875.

(31) (a) Tremel, W.; Yella, A.; Tahir, M. N.; Panthöfer, M.; Meuer, S.; Zentel, R. *Mater. Res. Soc. Symp. Proc.* **2009**, *1140*, PP07–01. (b) Shahar, C.; Levi, R.; Cohen, S. R.; Tenne, R. *J. Phys. Chem. Lett.* **2010**, *1*, 540–543.